

RESEARCH ARTICLE

A new *Xist* allele driven by a constitutively active promoter is dominated by *Xist* locus environment and exhibits the parent-of-origin effects

Yuko Amakawa^{1,*}, Yuka Sakata^{2,3,*}, Yuko Hoki², Satoru Arata⁴, Seiji Shioda⁴, Tatsuo Fukagawa¹, Hiroyuki Sasaki² and Takashi Sado^{2,3,‡}

ABSTRACT

The dosage difference of X-linked genes between the sexes in mammals is compensated for by genetic inactivation of one of the X chromosomes in XX females. A noncoding RNA transcribed from the *Xist* gene at the onset of X chromosome inactivation coats the X chromosome in cis and induces chromosome-wide heterochromatinization. Here, we report a new *Xist* allele (*Xist*^{CAG}) driven by a CAG promoter, which is known to be constitutively active in many types of cells. The paternal transmission of *Xist*^{CAG} resulted in the preferential inactivation of the targeted paternal X (Xp) not only in the extra-embryonic but also the embryonic lineage, whereas maternal transmission ended with embryonic lethality at the early postimplantation stage with a phenotype that resembled mutant embryos carrying a maternal deficiency in *Tsix*, an antisense negative regulator of *Xist*, in both sexes. Interestingly, we found that the upregulation of *Xist*^{CAG} in preimplantation embryos temporally differed depending on its parental origin: its expression started at the 4- to 8-cell stages when paternally inherited, and *Xist*^{CAG} was upregulated at the blastocyst stage when maternally inherited. This might indicate that the *Xist* locus on Xp is permissive to transcription, but the *Xist* locus on the maternal X (Xm) is not. We extrapolated from these findings that the maternal *Xist* allele might manifest a chromatin structure inaccessible by transcription factors relative to the paternal allele. This might underlie the mechanism for the maternal repression of *Xist* at the early cleavage stage when *Tsix* expression has not yet occurred on Xm.

KEY WORDS: X chromosome, Chromatin, Epigenetics, Mouse

INTRODUCTION

Among the many long noncoding RNAs (lncRNA) implicated in gene regulation, the X-inactive-specific transcript (*Xist*) is one of the most extensively studied lncRNAs and its biological significance has been well described (Brockdorff et al., 1992; Brown et al., 1991, 1992; Marahrens et al., 1997; Penny et al., 1996). *Xist* RNA plays an indispensable role in X chromosome inactivation (X-inactivation)

in female mammals, a process by which the dosage difference of X-linked genes between the sexes is compensated for by transcriptionally silencing one of the two X chromosomes during early development (Lyon, 1961). At the onset of X-inactivation, *Xist* becomes upregulated from one or the other X chromosome and its lncRNA associates in cis with the X chromosome from which it originates, to induce chromosome-wide heterochromatinization.

In the mouse, X-inactivation is imprinted in favor of the paternal X (Xp) in the extra-embryonic lineage, which gives rise to the placenta and some extra-embryonic membranes (Takagi and Sasaki, 1975), whereas it takes place in an essentially random fashion regardless of the parental origin in the embryonic lineage, which gives rise to all tissues of the fetus. *Xist* becomes monoallelically upregulated on Xp at the 4- to 8-cell stages and this paternal allele-specific expression is maintained in the trophectoderm and primitive endoderm of the blastocyst, both of which belong to extra-embryonic lineages. *Xist* clouds are lost in cells that have contributed to the epiblast lineage of the inner cell mass (ICM), and the previously inactivated Xp becomes transiently reactivated prior to the subsequent inactivation of either X in differentiating epiblast cells (Mak et al., 2004; Okamoto et al., 2004). Reactivation of the inactive X has also been observed in the primordial germ cells (PGCs) of female embryos (Monk and McLaren, 1981), which takes several days around the time they enter meiosis and accompanies the loss of *Xist* clouds (Sugimoto and Abe, 2007). The inactive X is thought to be reactivated for the proper progression of meiosis, especially for the pairing of two homologous X chromosomes in the prophase of meiosis I (Sugimoto and Abe, 2007). Although the downregulation of *Xist* has commonly been observed in the ICM and PGCs, to what extent they share the mechanism for reactivation is not clear. Williams et al. previously showed that reactivation of X-linked genes sometimes precedes the loss of *Xist* clouds in the ICM, which implies that the downregulation of *Xist* is not necessarily a primary cause of reactivation, at least in the ICM (Williams et al., 2011).

Although the biological significance of X-reactivation and of the accompanying downregulation of *Xist* in the ICM and PGCs have not been fully established, it is assumed that these events are associated with global reprogramming, which resets the previous epigenome in the ICM and PGCs and induces the expression of pluripotency factors including those reported to negatively regulate *Xist*, such as Oct3/4 (Pou5f1 – Mouse Genome Informatics), Sox2 and Nanog (Navarro et al., 2008). These factors may directly or indirectly downregulate *Xist*. A recent study, however, showed that the deletion of binding sites for these factors present in *Xist* intron 1 did not appear to affect this process in the ICMs (Minkovsky et al., 2013). A series of events in the process of reprogramming in addition to the expression of pluripotency factors might also

¹Division of Molecular Genetics, National Institute of Genetics, Research Organization of Information and Systems, 1111 Yata, Mishima 411-8540, Japan.

²Division of Epigenomics and Development, Medical Institute of Bioregulation, Kyushu-University, 3-1-1 Maidashi, Higashi-ku, Fukuoka 812-8582, Japan.

³Department of Advanced Bioscience, Graduate School of Agriculture, Kinki University, 3327-204, Nakamachi, Nara 631-8505, Japan. ⁴Department of Anatomy, Showa University School of Medicine, 1-5-8 Hatanodai, Shinagawa-ku, Tokyo 142-8555, Japan.

*These authors contributed equally to this work

‡Author for correspondence (tsado@nara.kindai.ac.jp)

contribute to the downregulation of *Xist* by causing changes in the chromatin structure of the *Xist* locus or the expression of transcription factors required for continuous *Xist* expression. Although the downregulation of *Xist* may not be a prerequisite for X-reactivation, as suggested by Williams et al. (2011), its biological significance cannot be addressed until the effect of continuous presence of *Xist* clouds in the ICMs and PGCs is examined.

In contrast to *Xist*, its antisense negative regulator, known as *Tsix*, is only expressed from the maternal X (Xm) from the morula/blastocyst stage until the midgestation stage in cells that maintain imprinted X-inactivation, namely in the extra-embryonic lineages (Lee, 2000; Sado et al., 2001). The targeted disruption of *Tsix*, when maternally inherited, was shown to result in the ectopic upregulation of normally silent maternal *Xist* and subsequent inactivation of Xm in the extra-embryonic lineages of both sexes, which demonstrated the antagonizing effect of *Tsix* on *Xist* in cis. Xm was shown to acquire an imprint during the prophase of meiosis I, which rendered Xm resistant against inactivation in the extra-embryonic lineages (Goto and Takagi, 1998; Tada et al., 2000; Takagi and Abe, 1990). By contrast, whether Xp possesses an imprint that facilitates its inactivation in the extra-embryonic lineages remains unclear. The maternal imprint by itself might be potentially sufficient enough to drive imprinted X-inactivation in these particular lineages by leaving Xp as the sole X capable of undergoing inactivation. As Xm carrying the *Tsix* deficiency has lost the ability to resist inactivation in the extra-embryonic tissues, *Tsix* expression could be considered to represent a primary output of the imprint laid on Xm. One can argue against this point of view, however, if the maternal imprint is supposed to be responsible for the repression of maternal *Xist* at the 4- to 8-cell stages as well because maternal *Tsix* has not yet been expressed at these stages.

In this study, we generated a new *Xist* allele (*Xist*^{CAG}) that was driven by a CAG promoter, which is considered one of the strongest and most ubiquitous promoters (Niwa et al., 1991). We expected that this allele, when paternally inherited, would allow us to unanimously inactivate the targeted Xp in the embryonic lineage by the constitutive expression of *Xist*^{CAG} upon the choice of X-inactivation and to also sustain *Xist* expression in the ICM and PGCs. By contrast, when maternally inherited, we expected that this allele would result in a phenocopy of embryos with maternal deletion of *Tsix* in both sexes. We found that *Xist*^{CAG} behaved as expected, except for the failure to sustain *Xist* clouds in the ICM and PGCs. Although the unexpected downregulation of *Xist*^{CAG} in these cells prevented further investigations into the effects of the continuous expression of *Xist* in cells undergoing reprogramming and X-reactivation, we identified interesting parental origin specific-differences in the timing of *Xist*^{CAG} upregulation in preimplantation embryos. Its expression started at the 4- to 8-cell stages when paternally inherited, whereas *Xist*^{CAG} was not upregulated until the blastocyst stage when maternally inherited. Here, we discussed what these results may indicate in terms of the differential regulation of *Xist* in preimplantation-stage embryos.

RESULTS

A new *Xist* allele driven by a CAG promoter was introduced into the mouse

A targeting vector was constructed to replace the endogenous *Xist* promoter with a cassette containing a CAG promoter (Niwa et al., 1991), which is known to be active in many types of cells including germ cells (Okabe et al., 1997; Sakai and Miyazaki, 1997), and a floxed selection marker (Fig. S1A). Following homologous recombination in embryonic stem cells (ESCs), those harboring

the mutant allele referred to as *Xist*^{CAG2L} were isolated (Fig. S1B). Because the transcription initiated from the CAG promoter could essentially be terminated by the presence of polyadenylation signals located 3' to the selection marker, we expected that the *Xist*^{CAG2L} allele would not produce functional *Xist* RNA and would behave in the same way as a null allele that was created previously (Marahrens et al., 1997). We therefore crossed the male chimeras with females heterozygous for the *Tsix* deletion ($\Delta Tsix$) (Sado et al., 2001) (see Materials and Methods) and successfully obtained female offspring carrying the *Xist*^{CAG2L} allele in combination with the $\Delta Tsix$ allele (Fig. S1C). They were subsequently crossed with males carrying a *Pgk2*-cre transgene (Kido et al., 2005), which allowed the expression of cre recombinase specifically in the spermatocyte under the control of the *Pgk2* promoter. We expected that males carrying *Xist*^{CAG2L} in combination with *Pgk2*-cre would transmit the *Xist*^{CAG} allele to female pups via cre-mediated conversion in the spermatocytes when crossed with wild-type females. As shown in Fig. S1D, we successfully recovered females heterozygous for *Xist*^{CAG}, which demonstrated that spermatogenesis was not compromised by the conversion of *Xist*^{CAG2L} into *Xist*^{CAG} in the spermatocytes. The presence of the respective alleles thus introduced into mice was confirmed by Southern blotting (Fig. S1C). A 197 bp portion surrounding the major transcription start site of *Xist* (chrX: 100,678,537–100,678,733 on mm9) was replaced with the CAG promoter in the *Xist*^{CAG} allele.

The X chromosome carrying the *Xist*^{CAG} allele was selectively inactivated in somatic cells

It was reasonable to expect the X chromosome undergoing inactivation to be confined to the wild-type X in *X*^{CAG2L}X females and the mutated *X*^{CAG} in *XX*^{CAG} females. (Throughout this article, the maternal X precedes the paternal one, and *X*^{CAG2L} and *X*^{CAG} refer to X chromosomes carrying *Xist*^{CAG2L} and *Xist*^{CAG}, respectively.) However, because RNA expressed from the *Xist*^{CAG} allele lacked the first 20 nucleotides present in wild-type *Xist* RNA and possessed an additional unrelated sequence derived from the CAG cassette instead, we examined whether these changes affected the function and processing of RNA produced from the *Xist*^{CAG} allele. We derived mouse embryonic fibroblasts (MEFs) heterozygous for the respective *Xist* mutations using mice with a Robertsonian translocation, Rb(X.9)6H, in which the X chromosome and chromosome 9 were fused at the centromere [*X*^{Rb(X.9)}] (Tease and Fisher, 1991). *X*^{CAG2L}*X*^{Rb(X.9)} and *X*^{Rb(X.9)}*X*^{CAG} MEFs thus derived allowed us to easily identify the mutated X by its morphology. We carried out RNA fluorescence *in situ* hybridization (RNA-FISH) to examine the expression of *Xist* in these mutant MEFs as well as in control *XX*^{Rb(X.9)} MEFs (Fig. S2A,B). The results demonstrated that whereas the *Xist*^{CAG2L} allele was functionally null and did not produce functional *Xist* RNA, the *Xist*^{CAG} allele constitutively expressed functional RNA coating the *X*^{CAG} in cis.

The nature of *Xist* RNA expressed from *X*^{CAG} in MEFs was examined by northern blotting. As shown in Fig. S2C, *X*^{CAG} produced apparently the same species of *Xist* RNA as the wild-type X, which indicated that there were no aberrant transcripts resulting from unexpected splicing or termination. The expression level of *Xist* in *XX*^{CAG} was, however, about tenfold higher than that in *XX*, which is consistent with the strong activity of the CAG promoter (Fig. S2C). We further compared the stability of the *Xist* RNA expressed from *X*^{CAG} with that from the wild-type X using *XX*^{CAG} and *XX* MEFs, and found that the half-life of RNA expressed from the *Xist*^{CAG} allele was essentially the same as that of wild-type *Xist* RNA (Fig. S2D).

As the inactive X is known to replicate late in the S phase of the cell cycle, we examined when replication of the respective X chromosomes occurred in these MEFs. In $XX^{Rb(X.9)}$ MEFs, the morphologically normal wild-type X replicated late in 58% of cells, whereas $X^{Rb(X.9)}$ did so in the remaining 42%, consistent with random X-inactivation. In mutant MEFs, by contrast, the late replicating X was confined to $X^{Rb(X.9)}$ in $X^{CAG2L} X^{Rb(X.9)}$ MEFs, and to X^{CAG} in $X^{Rb(X.9)} X^{CAG}$ MEFs (Fig. S2E,F). These results demonstrated that both mutations caused a skewing of inactivation in favor of the wild-type X in $X^{CAG2L} X$ and the mutated X in XX^{CAG} .

We further examined gene expression on X^{CAG2L} and X^{CAG} in MEFs prepared from F1 fetuses of the JF1 strain and respective mutant mice. These MEFs allowed us to study the allelic expression of X-linked genes and the result demonstrated that the genes on X^{CAG2L} were active, whereas those on X^{CAG} had been uniformly inactivated in the respective mutant MEFs (Fig. S2G). Taking all these results together, we concluded that both of the mutant alleles exerted the expected effect on the inactivation pattern of the X chromosome: the $Xist^{CAG2L}$ allele rendered X^{CAG2L} incompetent to undergo inactivation, whereas the $Xist^{CAG}$ allele constitutively produced functional RNA to silence the chromosome in cis.

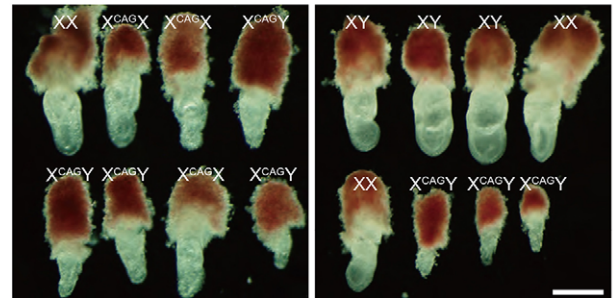
Maternal transmission of $Xist^{CAG}$ recapitulated the phenotype seen upon maternal transmission of the $Tsix$ mutation

Selective inactivation of a genetically manipulated X chromosome was shown to occur in the somatic cells of females heterozygous for X^{ATsix} of a paternal origin. Although these females were apparently normal, both male and female embryos conceived by them died *in utero* when X^{ATsix} was transmitted owing to the ectopic expression of maternal $Xist$ from the mutated X^{ATsix} in the extra-embryonic tissues after implantation (Lee, 2000; Sado et al., 2001). We crossed XX^{CAG} females and wild-type C57Bl/6 males to see if $Xist^{CAG}$ behaved in a manner similar to the $Tsix$ -deficient allele upon maternal transmission. Although XX^{CAG} females gave birth to healthy pups of both sexes, X^{CAG} had been barely transmitted to them, which suggested that most of the embryos that had inherited $Xist^{CAG}$ died *in utero* (Fig. 1A). In a single female survivor with maternal $Xist^{CAG}$, it is possible that the imprinted Xp inactivation in the extra-embryonic tissues was somehow reversed by shutting off paternal $Xist$ at the early postimplantation stage, allowing the embryo to survive despite the expression of maternal $Xist^{CAG}$. When embryos were dissected out at embryonic day (E) 7.5 from XX^{CAG} females, both $X^{CAG}X$ and $X^{CAG}Y$ embryos, although found at the expected ratio, were stunted with abnormal morphology, which was reminiscent of embryos carrying maternal X^{ATsix} (Fig. 1A,B). The distal part of these embryos, which was enriched with embryonic ectoderm, and their trophoblast were subsequently examined for $Xist$ expression by RNA-FISH. $X^{CAG}X$ embryos were manifested by single $Xist$ clouds in the embryonic ectoderm, but by two clouds in a large proportion of the nuclei in the trophoblast (Fig. 1C; Fig. 2B). The single clouds in the former were probably derived from maternal $Xist^{CAG}$. In $X^{CAG}Y$ embryos, single $Xist$ clouds were found in most of the nuclei in both tissues (Fig. 1C; Fig. 2B). These results demonstrated that X^{CAG} , when maternally inherited, recapitulated the behavior of the X deficient for $Tsix$. It is likely that the maternal transmission of $Xist^{CAG}$ caused embryonic lethality owing to functional nullisomy of the X chromosome in the extra-embryonic lineage of $X^{CAG}X$ embryos and in both embryonic and extra-embryonic lineages of $X^{CAG}Y$ embryos.

A

$XX^{CAG} \times XY$					
	XX	$X^{CAG}X$	XY	$X^{CAG}Y$	total/ litters
No. of pups 3-week	71 (46.4%)	1 (0.7%)	81 (52.9%)	0 (0%)	153/ 32
No. of E7.5 embryos	10 (20.4%)	13 (26.5%)	14 (28.6%)	12 (24.5%)	49/ 8

B



C

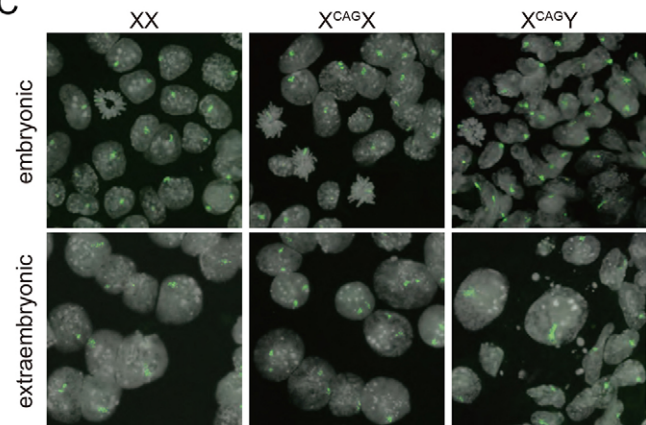


Fig. 1. The phenotype of the embryos carrying maternal $Xist^{CAG}$ mimics the phenotype of the mutant embryos carrying a maternal deficiency in $Tsix$. (A) The number of pups and E7.5 embryos recovered from a cross between XX^{CAG} females and wild-type males. $Xist^{CAG}$, although found at the Mendelian ratio when examined at E7.5, was transmitted to few live pups from the mother. (B) Examples of the gross morphology of E7.5 embryos recovered from XX^{CAG} females sired by wild-type males. The genotype of each embryo is indicated. Scale bar: 500 μ m. (C) $Xist$ expression detected by RNA-FISH (green) in the embryonic and extra-embryonic tissues (trophoblast) of XX, $X^{CAG}X$ and $X^{CAG}Y$ embryos recovered at E7.5.

Maternal $Xist^{CAG}$ was not upregulated until the peri-implantation stage

$X^{CAG}X$ and $X^{CAG}Y$ embryos, although stunted, apparently had undergone gastrulation. We reasoned that if maternal X^{CAG} became silenced during the preimplantation stages, these mutants would have suffered from the functional nullisomy of the X chromosome and would not have survived until the gastrulation stage. To investigate when maternal $Xist^{CAG}$ became upregulated and formed the cloud in $X^{CAG}X$ and $X^{CAG}Y$ embryos during development, we carried out RNA-FISH using embryos recovered at earlier stages from XX^{CAG} females crossed with wild-type males. The sex of each embryo was subsequently identified by Y chromosome painting (the results of Y-painting were noted visually after staining, but were not recorded as image data). $Xist$ expression was examined in 15 female and 15 male 8-cell-stage embryos recovered at E2.5. We found that whereas the nuclei of one class of female embryos contained only a single large $Xist$ cloud, those of the other class



contained very faint scattered signals in addition to a large *Xist* cloud (Fig. 2A,B; Fig. S3). Similarly, the nuclei of half of the male embryos were negative for *Xist*, whereas those of the remaining half contained very faint scattered signals (Fig. 2A,B; Fig. S3). Although we could not verify the genotype of the embryos, we suspected that the very faint scattered signals represented very weak expression of *Xist*^{CAG}, which contrasted well with the intense signal of the *Xist* cloud in females. When E3.5 blastocysts were examined, a small subset of the nuclei in 3/7 females and 6/11 males contained two and one *Xist* cloud(s), respectively (Fig. 2A,B). It would be reasonable

to assume that they represented $X^{CAG}X$ and $X^{CAG}Y$ embryos, respectively. It is, therefore, likely that maternal $Xist^{CAG}$ had not been fully upregulated in the majority of the blastomeres at this stage. This contrasted well with female blastocysts carrying $Xist^{CAG}$ on Xp (XX^{CAG}), which exhibited clear single $Xist$ clouds in a large proportion of the nuclei (Fig. 3A). In fact, $Xist^{CAG}$ in every blastomere of XX^{CAG} embryos ($n=3$) had been upregulated in the same manner as $Xist$ on Xp in wild-type female embryos by the 8-cell stage (Fig. 3A). The prevalence of the nuclei containing an extra $Xist$ cloud, although increased to some extent, was still as low

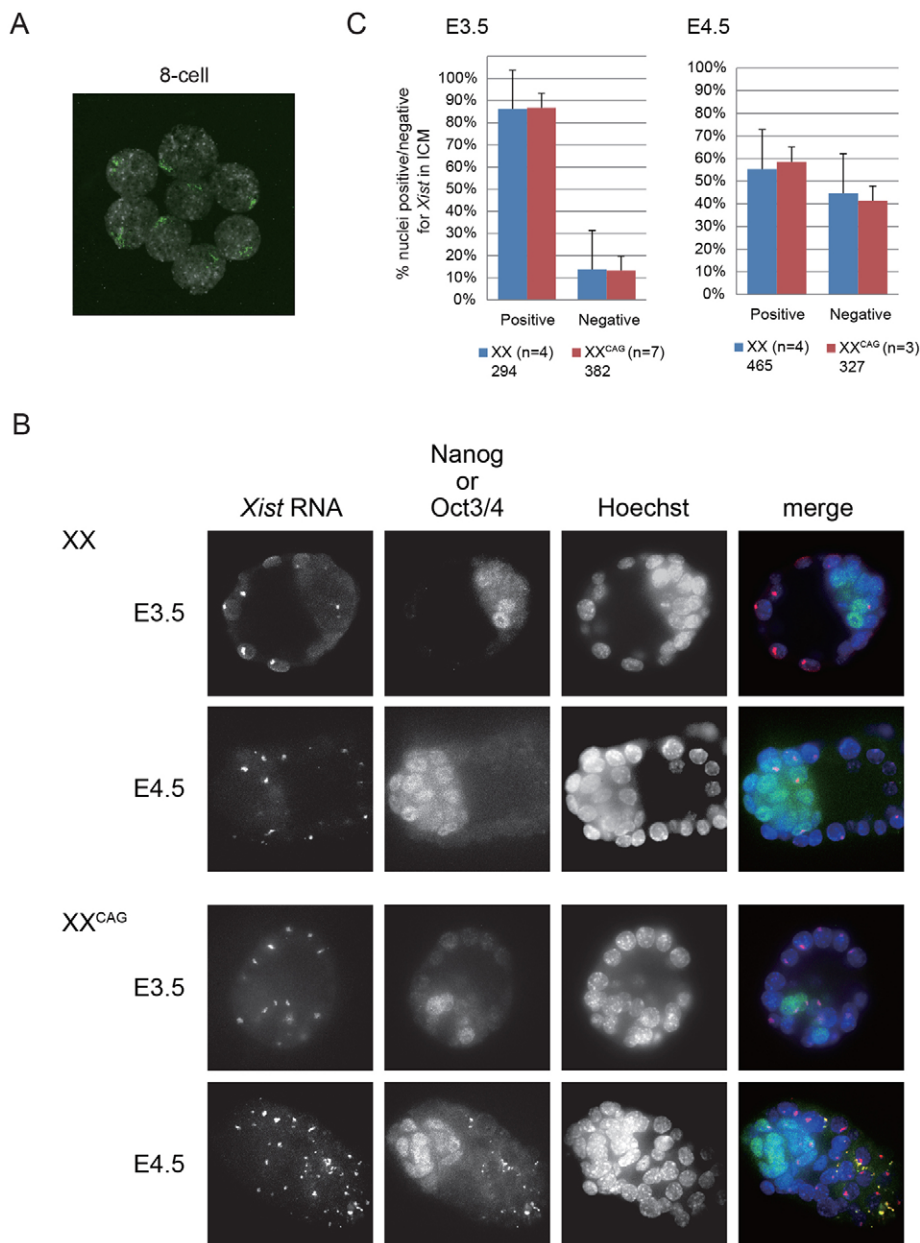


Fig. 3. *Xist*^{CAG} on the paternal X was downregulated in the ICM. (A) *Xist* expression detected by RNA-FISH in an XX^{CAG} embryo at the 8-cell stage. (B) Immuno-RNA-FISH detecting *Xist* and ICM lineage markers, either Nanog (E3.5) or Oct3/4 (E4.5), in XX and XX^{CAG} blastocysts recovered at E3.5 and E4.5. (C) Graphs show the percentage of nuclei positive and negative for the *Xist* cloud among cells positive for Nanog (E3.5) or Oct3/4 (E4.5) in XX and XX^{CAG} blastocysts recovered at E3.5 and E4.5. *n* indicates the number of embryos examined. The number of nuclei examined are shown below the graph legend. Error bars represent s.d.

as 20% in presumptive X^{CAG}X and X^{CAG}Y embryos recovered at E4.5, but reached a level comparable to that seen in the embryonic and extra-embryonic tissues of E7.5 mutant embryos by E6.5 (Fig. 2B). These results demonstrated that the timing of *Xist*^{CAG} upregulation differed depending on its parental origin and, when maternally inherited, it started to be expressed at around the blastocyst stage despite the allele being under the control of the CAG promoter. It is likely that ectopic inactivation of X_m did not take place until around the time of implantation in X^{CAG}X and X^{CAG}Y embryos. This is again reminiscent of the timing when X_m carrying the *Tsix* deficiency started to be ectopically inactivated (Sado et al., 2001).

***Xist*^{CAG} on the paternal X was downregulated in the ICM**

Paternal *Xist* upregulated in every blastomere of the female embryos during the early cleavage stages was shown to be silenced in cells contributing to a part of the ICM (Mak et al., 2004; Okamoto et al., 2004). This accompanied transient reactivation of the hitherto

inactive X_p prior to the onset of random X-inactivation taking place in the epiblast lineage. It was of interest whether the expression of *Xist*^{CAG} inherited from the father, which was initiated at around the 4- to 8-cell stages, was sustained in cells allocated to the ICM with respect to understanding the biological significance of *Xist* downregulation in X_p reactivation and the reprogramming of cells in the ICM. Accordingly, we carried out RNA-FISH for *Xist* expression in combination with immunostaining for ICM lineage-specific markers, either Nanog or Oct3/4, using blastocysts recovered from wild-type females crossed with [X^{CAG2LY}; *Pgk2-cre*] males in comparison with wild-type. Among the cells positive for Nanog, ~10% had already lost *Xist* clouds in E3.5 wild-type blastocysts. Contrary to our expectation, the proportion of those negative for *Xist* were comparable in XX^{CAG} blastocysts and wild-type blastocysts recovered at E3.5 (Fig. 3B,C). When examined at E4.5, the population of cells negative for *Xist* RNA had become >40% of those positive for Oct3/4 in both cases (Fig. 3B,C). It was likely, therefore, that *Xist*^{CAG} upregulated by the 8-cell stage failed

to sustain its expression in a subset of ICM cells. These results suggested that paternally derived *Xist*^{CAG}, although driven by the CAG promoter, was downregulated in the epiblast lineage in a manner similar to that in wild-type. Although unexpected silencing of *Xist*^{CAG} precluded a further analysis for the effect of the continuous association of *Xist* RNA with Xp on X-reactivation and the reprogramming in the ICM, it raised an interesting possibility that a mechanism involved in the repression of the endogenous *Xist* promoter on Xp in the epiblast lineage might also be effective on the CAG promoter.

The expression of *Xist*^{CAG} in PGCs was not sustained throughout oogenesis in *XX*^{CAG} fetuses

Reactivation of the inactive X also takes place in PGCs around the time when PGCs enter meiosis. *Xist* clouds are known to be lost in PGCs by E10.5 prior to reactivation of the inactive X (de Napoles et al., 2007; Sugimoto and Abe, 2007). In *XX*^{CAG} female embryos, *X*^{CAG} should have been uniformly inactivated in every cell including PGCs by the constitutive expression of *Xist*^{CAG}. Gonads isolated from E10.5, E13.5 and E16.5 embryos were trypsinized and the cell suspension containing germ cells and the surrounding somatic cells was cytospun onto a slide for RNA-FISH. A GFP transgene driven by the Oct3/4 promoter (Yoshimizu et al., 1999) was introduced into the embryos so that germ cells could be identified by immunostaining with an antibody against GFP. As shown in Fig. 4A,B, *Xist* RNA disappeared in most of the wild-type PGCs by E10.5, which is consistent with previous studies. By contrast, >70% of PGCs still retained *Xist* RNA on *X*^{CAG}, although this was lower than that of the surrounding somatic cells, in *XX*^{CAG} embryos at E10.5 (Fig. 4A,B). Although we expected that *Xist* RNA might remain on *X*^{CAG} in germ cells throughout development, the population of germ cells positive for *Xist* RNA declined over time to 20% at E13.5 and 0.4% at E16.5 in *XX*^{CAG} embryos. As a significant difference in the number of germ cells was not observed between wild-type and *XX*^{CAG} embryos at each stage examined, the reduction in the number of germ cells positive for *Xist* RNA was unlikely to be due to elimination by cell death, but was attributable to the downregulation of *Xist*^{CAG}. We carried out qRT-PCR to examine the expression levels of *Xist* RNA in PGCs isolated from E13.5 *XX* and *XX*^{CAG} gonads. As shown in Fig. 4C, the relative abundance of *Xist* RNA stably present in PGCs was markedly lower than that in the surrounding somatic cells of the gonads in both *XX* and *XX*^{CAG} fetuses. This suggests that the absence of *Xist* clouds in RNA-FISH experiments was not due to a loss of localization to the inactive X. As was the case in the ICM, a mechanism that silences the endogenous *Xist* promoter in PGCs appeared to be effective on the CAG promoter.

The CAG promoter was not methylated in PGCs that had lost *Xist*^{CAG} expression

It was unexpected that the CAG promoter could not sustain *Xist*^{CAG} expression in the ICM and PGCs, given the fact that many transgenes driven by the CAG promoter are expressed in the ICM and PGCs. As the unexpected silencing of transgenes is often associated with promoter methylation, we carried out bisulfite sequencing to examine the methylation levels of the 16 and 59 CpG sites in the endogenous *Xist* promoter and CAG promoter, respectively, in E13.5 PGCs isolated from *XX* and *XX*^{CAG} gonads by fluorescence-activated cell sorting (FACS) using the GFP transgene driven by the Oct3/4 promoter. In the gonads of *XX* females, the *Xist* promoter was methylated at ~40% in somatic cells surrounding PGCs, consistent with the *Xist* promoter in somatic cells being methylated on the active X and unmethylated on the

inactive X (Fig. 5A) (McDonald et al., 1998; Norris et al., 1994). Interestingly, this region was essentially unmethylated in PGCs, which suggests the possibility that *Xist* was downregulated in PGCs by either a mechanism independent of promoter methylation if at the transcriptional level or post-transcriptional processing of *Xist* RNA.

The *Xist* promoter on the wild-type X was markedly methylated in the gonads of *XX*^{CAG} females, whereas the CAG promoter on *X*^{CAG} was unmethylated in somatic cells (Fig. 5B). Interestingly, as was the case in *XX* germ cells, the endogenous *Xist* promoter on the wild-type X and the CAG promoter on *X*^{CAG} were both essentially unmethylated in *XX*^{CAG} PGCs. This suggests that the eventual downregulation of the *Xist*^{CAG} allele in *XX*^{CAG} PGCs was not mediated by promoter methylation. As was the case in the ICM, the *Xist*^{CAG} allele appeared to be repressed in the same manner as endogenous *Xist* in the PGCs of wild-type females.

DISCUSSION

The reversal of the inactive X chromosome is observed in two different phases in the mouse life cycle. It occurs in cells that have contributed to the ICM in the blastocyst and also in PGCs around the time when they enter meiosis; however, whether the underlying mechanism is common between these cell types is unknown. As reactivation in both cases accompanied the downregulation of *Xist*, it has been presumed that the loss of *Xist* RNA might be causally involved in reactivation. A previous study by Williams et al. (2011), however, showed that the reactivation of genes on the inactivated Xp sometimes preceded the disappearance of an *Xist* cloud in a subset of cells in the ICM, which suggested that X-reactivation was not necessarily coupled with the loss of *Xist* RNA in the ICM. We assumed that the *Xist*^{CAG} allele would allow us to address the effect of the continuous association of *Xist* RNA with the X chromosome on X-reactivation and the subsequent reprogramming if its expression was sustained in the ICM and PGCs. The results were as expected in somatic cells and its phenotype upon maternal transmission mimicked the phenotype caused by a maternal deficiency in *Tsix*; however, cells in neither the ICM nor PGCs sustained an *Xist* cloud formed by the expression of *Xist*^{CAG}. Although this was unexpected given the fact that the *Xist*^{CAG} allele was driven by the CAG promoter, which is known to be active in many types of cells including those of the ICM and PGCs, these results may imply that even the heterologous CAG promoter, when placed in the context of the *Xist* locus, comes to be under the control of the same regulatory mechanism as the endogenous *Xist* promoter. Given the fact that the CAG promoter has been replaced with a 197 bp region surrounding the major transcription start site of *Xist*, it is likely that the element crucial for the presumed regulatory mechanism for the *Xist* promoter resides outside the replaced region. It is important to note that both male and female ESCs carrying *Xist*^{CAG} could be efficiently derived from blastocysts and that *Xist*^{CAG} in such ESCs became upregulated to form an *Xist* cloud only upon induction of differentiation (Fig. S4), further suggesting that the CAG promoter behaved in a way similar to the endogenous *Xist* promoter.

Although the transcription of *Xist* has been correlated with the methylation status of CpG sites in the *Xist* promoter in somatic cells (Norris et al., 1994), DNA methylation does not seem to be involved in the repression of *Xist* at the blastocyst stage as the *Xist* promoter is essentially unmethylated in blastocysts and isolated ICM cells (McDonald et al., 1998). This also appeared to be the case in PGCs as the *Xist* promoter in E13.5 PGCs, in which an *Xist* cloud essentially disappeared by E10.5, was largely devoid of DNA methylation. It is tempting to speculate that the presumptive

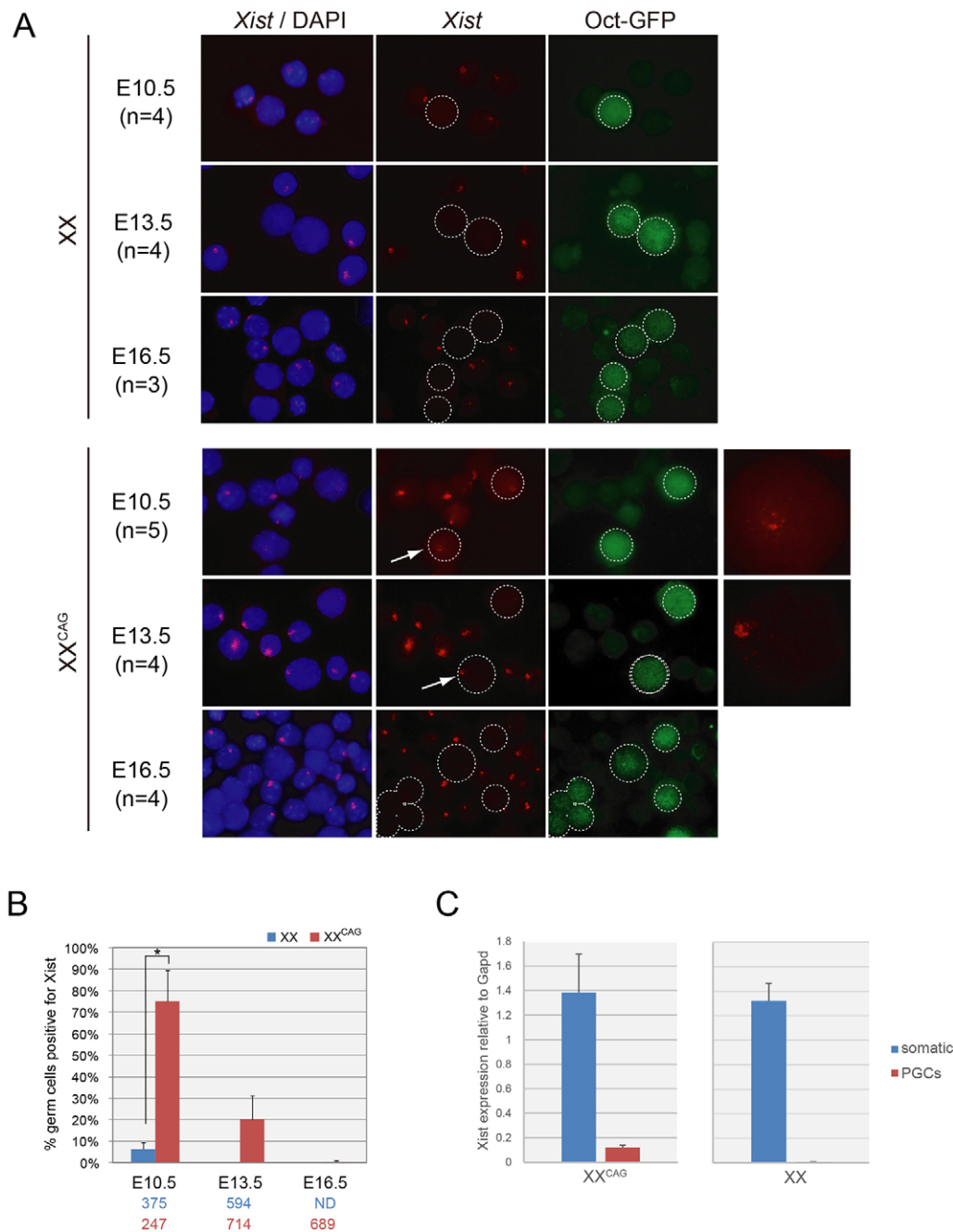


Fig. 4. Prolonged expression of *Xist* in the germ cells of XX^{CAG} females. (A) *Xist* expression detected by immuno-RNA-FISH in the fetal gonads. *Xist* RNA (red) was detected by RNA-FISH in the gonads of XX and XX^{CAG} females (E10.5–E16.5). Germ cells were identified by the expression of an Oct3/4-GFP transgene, which was specifically expressed in germ cells. The nucleus indicated by an arrow in XX^{CAG} (E10.5 and E13.5) is shown at a higher magnification on the right. *Xist* coating was evident in these germ cell nuclei. DNA was counterstained with DAPI (blue). Germ cells are marked with dotted circles. (B) Summary of the immuno-RNA-FISH analysis in germ cells. The graph shows the prevalence of germ cells positive for *Xist* RNA. * $P < 0.01$ (t -test). Error bars represent s.d. The numbers of cells examined are shown below the graph: blue, XX; red, XX^{CAG}. (C) qRT-PCR analysis of *Xist* expression in PGCs isolated from the surrounding somatic cells of E13.5 XX and XX^{CAG} gonads by FACS. Error bars represent s.d.

regulatory mechanism, which makes the *Xist* promoter transcriptionally inert in the ICM and PGCs in a manner independent of DNA methylation, also effectively operates upon the CAG promoter residing at the *Xist* locus and downregulates *Xist*^{CAG} in the ICM and PGCs of XX^{CAG} embryos. Among the mutated *Xist* alleles so far introduced into the mouse, that reported by Nesterova et al. (2003), which causes skewed X-inactivation due to selective expression of the targeted alleles, and that reported by Savarese et al. (2006), which is driven by a tetracyclin-inducible

promoter, would be of interest to see the behavior of their heterologous promoter at the *Xist* locus in the ICM and PGCs. The latter allele can be upregulated in undifferentiated ESCs if doxycycline (dox) is administered, whereas the *Xist*^{CAG} allele is not as long as the cells are maintained in an undifferentiated state. The presence of abundant transactivator in the dox-inducible cells might explain the difference in the action between these two alleles in undifferentiated ESCs. Nonetheless, it should be mentioned that we could not formally rule out the possibility that *Xist* clouds were lost

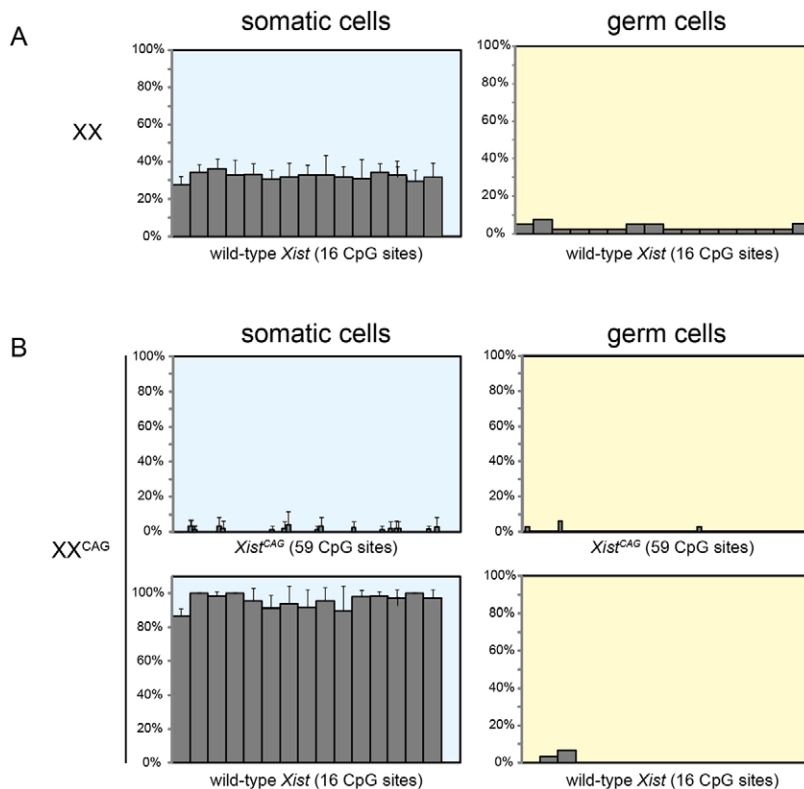


Fig. 5. Methylation levels of the *Xist* and CAG promoters in PGCs. (A,B) The methylation status of the 16 and 59 CpG sites present in the 5' region of the endogenous *Xist* (A) and CAG promoters (B), respectively, was analyzed in PGCs recovered from XX and XX^{CAG} fetuses at E13.5 by bisulfate sequencing. PGCs isolated by FACS were used for the assay. Error bars represent s.d.

in the ICM and PGCs as a result of an alternative mechanism that abolishes the stability of *Xist* RNA rather than transcriptional repression.

This study also provided another important implication for the asymmetric expression of *Xist* between Xp and Xm in preimplantation embryos. The timing by which *Xist*^{CAG} became upregulated was significantly different depending on its parental origin. Upon paternal transmission, a single *Xist* cloud derived from *Xist*^{CAG} became evident by the 8-cell stage, which was similar to wild-type XX embryos, whereas an extra *Xist* cloud originating from maternally inherited *Xist*^{CAG} in X^{CAG}X and X^{CAG}Y embryos appeared in a subset of cells at the blastocyst stage. This may be attributed to the difference in the chromatin structure at the *Xist* locus between Xp and Xm derived from a spermatozoon and oocyte, respectively, in the early cleavage stages of embryos. As the paternal genome undergoes global remodeling of the chromatin soon after fertilization, it may be reasonable to assume that this paternal genome-specific event rendered the *Xist* locus on Xp more permissive to transcription than that on Xm. If the chromatin structure of the maternal *Xist* locus needs further cell division to become similar to that of the paternal locus, this would account for the lag in the timing of maternal *Xist*^{CAG} being upregulated relative to paternal *Xist*^{CAG}. Such a difference in the chromatin structure, if any, may also be relevant to the monoallelic upregulation of *Xist* in wild-type female embryos in favor of the paternal allele during preimplantation development (Sado and Sakaguchi, 2013). In other words, the maternal *Xist* allele was repressed during early cleavage stages because it was not yet ready for transcription owing to the compact chromatin structure being inaccessible by transcription factors. Given that the very weak scattered signals of *Xist* were observed from maternally inherited *Xist*^{CAG}, one might raise an alternative possibility that the maternal X chromosome is incompetent for *Xist*-coating at the early preimplantation stage.

Xist-coating detected in parthenogenetically activated embryos, however, argue against this. Recently, Fukuda et al. demonstrated that overexpression of Kdm4b, a histone demethylase for H3K9me3, can induce upregulation of *Xist* from the 4-cell stage in parthenogenetically activated embryos (Fukuda et al., 2014). This suggests, in fact, that global demethylation of H3K9me3 and subsequent alteration of the chromatin structure facilitate derepression of *Xist* on Xm otherwise repressed. This is apparently consistent with the idea that maternal *Xist* is repressed in the early preimplantation embryo primarily owing to the chromatin structure impermissive for transcription. An earlier work demonstrated that *Xist* expression occurs at the morula/blastocyst stage even in parthenogenones or gynogenones (Kay et al., 1994; Matsui et al., 2001; Nesterova et al., 2001). Although it was originally suggested that this represented erasure of the maternal imprint responsible for *Xist* silencing by the morula/blastocyst stage, it could be also explained as a result of several rounds of replication or cell division, which could have made the chromatin structure at the maternal *Xist* locus transcriptionally permissive.

It has been well accepted that an imprint laid on Xm during the prophase of meiosis I makes Xm resistant to inactivation in extra-embryonic lineages (Goto and Takagi, 1998; Tada et al., 2000). As a maternal deficiency in *Tsix* leads to the ectopic expression of maternal *Xist* in cis and the subsequent inactivation of Xm in extra-embryonic lineages (Lee, 2000; Sado et al., 2001), the monoallelic expression of maternal *Tsix* appears to be, at least in part, responsible for the output of the imprint laid on Xm. However, one can argue against this, given that maternal *Xist* is repressed at the early preimplantation stages, when *Tsix* has not yet been expressed. Our findings, however, suggest that the reason why the maternal *Xist*^{CAG} allele is less effectively transcribed than the paternal one at the early preimplantation stage might be because the chromatin state or structure of the *Xist* locus on Xm at that time is not ready for

robust transcription. If maternal *Xist* is repressed simply because the chromatin structure is inaccessible to transcription factors, one may not need to assume a germline imprint that prevents the upregulation of maternal *Xist* during the early cleavage stages. In other words, whether or not the maternal *Xist* is transcribed at the early preimplantation stage may not be a matter of a conventional imprint, such as differential methylation, but rather simply related to the chromatin state or structure. As *Tsix* starts to be monoallelically expressed from Xm at around the morula/blastocyst stages, *Tsix* would be able to block upregulation of maternal *Xist* thereafter if the presumptive transcriptionally incompetent chromatin structure at the *Xist* locus on Xm lasts for a few rounds of cleavage until the morula stage. It should be noted that the transcription of *Xist*^{CAG} appears to dominate the repressive effect of *Tsix* on Xm as *Xist*^{CAG} is upregulated from the blastocyst stage onwards.

MATERIALS AND METHODS

Generation of mice carrying *Xist*^{CAG}

The targeting vector, pCAG- Δ M20, was constructed as described in supplementary materials and methods, and introduced into J1 ESCs (Li et al., 1992). Of the 464 colonies picked up, 11 harbored the expected homologous recombination (*Xist*^{CAG2L}). Chimeric males were crossed with females heterozygous for the *Tsix*-deficient X (XX ^{Δ Tsix}) (Sado et al., 2001) to facilitate the transmission of Xp carrying the *Xist*^{CAG2L} allele (X^{CAG2L}) to female offspring as previously shown (Hoki et al., 2009; Ohhata et al., 2008; Sado et al., 2005, 2006). Females thus generated (X ^{Δ Tsix}X^{CAG2L}) were crossed with wild-type males to obtain X^{CAG2L}-X and X^{CAG2L}-Y. The floxed puromycin-resistance gene was removed through the male germline using a *Pgk2-cre* transgene to derive females heterozygous for *Xist*^{CAG} (XX^{CAG}). All mice were maintained and used in accordance with the Guidelines for the Care and Use of Laboratory Animals of Kinki University (KDAS-26-0006). MEFs were prepared as described in supplementary materials and methods.

RNA-FISH and chromosome painting

A DNA probe for RNA-FISH was prepared from 1 μ g of pR97E1 (Sado et al., 1996), a plasmid containing an *Xist* cDNA fragment, by nick translation using the Nick Translation Kit (Abbott) and either Cy3-dUTP (GE Healthcare) or green-dUTP (Abbott).

Chromosome spreads of MEFs were prepared by a standard air-dry method, and cytological preparations of blastocysts and postimplantation embryos were made as described by Okamoto et al. (2000) and Takagi et al. (1982), respectively. RNA-FISH was performed as described previously (Sado et al., 2001). Following examination of the *Xist* signal, chromosome painting was carried out to distinguish the morphologically normal X and X^{Rb(X,9)} (Tease and Fisher, 1991) using painting probes for chromosome X and chromosome 9 (Cambio) according to the manufacturer's instructions. The gender of blastocysts was identified using a painting probe for the Y chromosome after RNA-FISH.

Analysis of replication timing

Cells were incorporated with 5-bromo-2'-deoxyuridine (BrdU) for 8 h and chromosome spreads were subsequently prepared by a standard air-drying method for staining with Acridine Orange. The late-replicating inactive X chromosome was identified as a pale chromosome by this method.

RNA half-life assay

MEFs were seeded onto dishes and cultured overnight. The medium was replaced with that containing 50 μ g/ml 5,6-dichloro-1- β -D-ribofuranosyl benzimidazole (DRB; Calbiochem) on the following day and cells were collected every 3 h and lysed in ISOGEN (Wako). Five-hundred nanograms of total RNA isolated at each time point was converted into cDNA as described below. Real-time PCR was carried out for the quantification of *Xist* RNA at each time point using primers XistEx7F21 and XistEx7R20. The level of *Xist* RNA was normalized relative to that of 18S ribosomal RNA amplified using primers 18SRNA1 and 18SRNA2. The abundance of

the respective RNA at each time point was shown as a value relative to the abundance at 3 h after the addition of DRB.

Allelic expression analysis by RT-PCR

Following the DNase I treatment, RNA prepared from MEFs was converted into cDNA using the Prime Script 1st Strand cDNA Synthesis Kit (Takara) with random hexamer as a primer. PCR was carried out using primers specific for each of the X-linked genes, and amplified products were subsequently digested with appropriate restriction enzymes as described (Kalantry et al., 2009; Sugimoto and Abe, 2007).

Immuno-FISH

Blastocysts recovered at E3.5 and E4.5 were fixed in 4% paraformaldehyde containing 0.1% Triton X-100 for 10 min and subjected to hybridization with an *Xist* probe overnight. Following serial washes, embryos were postfixed with 4% paraformaldehyde and subjected to immunostaining using antibodies against either Nanog (Yamaguchi et al., 2009; 1:250) or Oct3/4 (N-19) (Santa Cruz, sc8628; 1:400), which were visualized by secondary antibodies, Alexa488-conjugated anti-rabbit IgG (Life Technologies, A-11034; 1:1000) for Nanog or Alexa488-conjugated anti-goat IgG (Life Technologies, A-11055; 1:1000) for Oct3/4.

Gonads isolated from E10.5, E13.5 and E16.5 female fetuses carrying an Oct3/4-GFP transgene (Yoshimizu et al., 1999) were trypsinized and the resultant suspension was subjected to a hypotonic treatment in 75 mM KCl for 10 min and fixed in 2% paraformaldehyde for 10 min on ice. Cells were cytospun for 10 min at 800 rpm (Cytospin 2, Shandon), permeabilized with 0.5% Triton X-100 in PBS for 5 min, and washed with PBS for 5 min. Following hybridization with an *Xist* probe and washing, cells were stained with an anti-GFP rat monoclonal antibody (Nacalai, 04404-26; 1:100) and an Alexa488-conjugated anti-rat IgG (Life Technologies, A-11006; 1:1000). Images were captured using either an Andor iXon^{EM} CCD camera or an Olympus DP70 color CCD camera.

Bisulfite sequencing

Genomic DNA prepared from PGCs at E13.5 was treated with bisulfite and purified using the Bisulfite Kit (TOYOBO) and EZ Kit (Zymo Research), respectively. Two-round PCR was carried out using semi-nested primers. First round PCR was carried out for 25 cycles with 8 ng of DNA using primers Bx-CAG1113F and Bx-CAG1686R for the CAG promoter, and XistPr2 and XistPr3 for the *Xist* promoter. Second round PCR was performed for 25–30 cycles with one-twentieth of the reaction from first round PCR using primers Bx-CAG1113F and Bx-CAG1646R for the CAG promoter, and XistPr2 and XistPr4 for the *Xist* promoter. The PCR products were subsequently cloned into the pGEM-Teasy vector (Promega) and sequenced.

Primers

Primer sequences used in this study are described in supplementary materials and methods.

Acknowledgements

We would like to thank Hitoshi Niwa for providing the plasmid containing the CAG promoter. We would also like to thank Hirosuke Shiura for technical advice on immuno-RNA-FISH of blastocysts; Takashi Tada for the kind gift of an anti-Nanog antibody; and Minako Kanbayashi and Michiko Arai for maintenance of the mouse colonies.

Competing interests

The authors declare no competing or financial interests.

Author contributions

Y.S. and Y.A. performed the experiments with the assistance of Y.H., analyzed the data, and edited the manuscript; H.S. and T.F. analyzed the data; S.A. and S.S. generated *Pgk2-cre* mice; T.S. designed the study, performed experiments and wrote the manuscript.

Funding

This work was supported by the Japan Society for the Promotion of Science KAKENHI [25291079 and 26116515 to T.S.].

Supplementary information

Supplementary information available online at
<http://dev.biologists.org/lookup/suppl/doi:10.1242/dev.128819/-DC1>

References

- Brockdorff, N., Ashworth, A., Kay, G. F., McCabe, V. M., Norris, D. P., Cooper, P. J., Swift, S. and Rastan, S.** (1992). The product of the mouse Xist gene is a 15 kb inactive X-specific transcript containing no conserved ORF and located in the nucleus. *Cell* **71**, 515–526.
- Brown, C. J., Ballabio, A., Rupert, J. L., Lafreniere, R. G., Grompe, M., Tonlorenzi, R. and Willard, H. F.** (1991). A gene from the region of the human X inactivation centre is expressed exclusively from the inactive X chromosome. *Nature* **349**, 38–44.
- Brown, C. J., Hendrich, B. D., Rupert, J. L., Lafrenière, R. G., Xing, Y., Lawrence, J. and Willard, H. F.** (1992). The human XIST gene: analysis of a 17 kb inactive X-specific RNA that contains conserved repeats and is highly localized within the nucleus. *Cell* **71**, 527–542.
- de Napoles, M., Nesterova, T. and Brockdorff, N.** (2007). Early loss of Xist RNA expression and inactive X chromosome associated chromatin modification in developing primordial germ cells. *PLoS ONE* **2**, e860.
- Fukuda, A., Tomikawa, J., Miura, T., Hata, K., Nakabayashi, K., Eggan, K., Akutsu, H. and Umezawa, A.** (2014). The role of maternal-specific H3K9me3 modification in establishing imprinted X-chromosome inactivation and embryogenesis in mice. *Nat. Commun.* **5**, 5464.
- Goto, Y. and Takagi, N.** (1998). Tetraploid embryos rescue embryonic lethality caused by an additional maternally inherited X chromosome in the mouse. *Development* **125**, 3353–3363.
- Hoki, Y., Kimura, N., Kanbayashi, M., Amakawa, Y., Ohhata, T., Sasaki, H. and Sado, T.** (2009). A proximal conserved repeat in the Xist gene is essential as a genomic element for X-inactivation in mouse. *Development* **136**, 139–146.
- Kalantry, S., Purushothaman, S., Bowen, R. B., Starmer, J. and Magnuson, T.** (2009). Evidence of Xist RNA-independent initiation of mouse imprinted X-chromosome inactivation. *Nature* **460**, 647–651.
- Kay, G. F., Barton, S. C., Surani, M. A. and Rastan, S.** (1994). Imprinting and X chromosome counting mechanisms determine Xist expression in early mouse development. *Cell* **77**, 639–650.
- Kido, T., Arata, S., Suzuki, R., Hosono, T., Nakanishi, Y., Miyazaki, J.-i., Saito, I., Kuroki, T. and Shioda, S.** (2005). The testicular fatty acid binding protein PERF15 regulates the fate of germ cells in PERF15 transgenic mice. *Dev. Growth Differ.* **47**, 15–24.
- Lee, J. T.** (2000). Disruption of imprinted X inactivation by parent-of-origin effects at Tsix. *Cell* **103**, 17–27.
- Li, E., Bestor, T. H. and Jaenisch, R.** (1992). Targeted mutation of the DNA methyltransferase gene results in embryonic lethality. *Cell* **69**, 915–926.
- Lyon, M. F.** (1961). Gene action in the X-chromosome of the mouse (*Mus musculus* L.). *Nature* **190**, 372–373.
- Mak, W., Nesterova, T. B., de Napoles, M., Appanah, R., Yamanaka, S., Otte, A. P. and Brockdorff, N.** (2004). Reactivation of the paternal X chromosome in early mouse embryos. *Science* **303**, 666–669.
- Marahrens, Y., Panning, B., Dausman, J., Strauss, W. and Jaenisch, R.** (1997). Xist-deficient mice are defective in dosage compensation but not spermatogenesis. *Genes Dev.* **11**, 156–166.
- Matsui, J., Goto, Y. and Takagi, N.** (2001). Control of Xist expression for imprinted and random X chromosome inactivation in mice. *Hum. Mol. Genet.* **10**, 1393–1401.
- McDonald, L. E., Paterson, C. A. and Kay, G. F.** (1998). Bisulfite genomic sequencing-derived methylation profile of the xist gene throughout early mouse development. *Genomics* **54**, 379–386.
- Minkovsky, A., Barakat, T. S., Sellami, N., Chin, M. H., Gunhanlar, N., Gribnau, J. and Plath, K.** (2013). The pluripotency factor-bound intron 1 of xist is dispensable for x chromosome inactivation and reactivation in vitro and in vivo. *Cell Rep.* **3**, 905–918.
- Monk, M. and McLaren, A.** (1981). X-chromosome activity in foetal germ cells of the mouse. *J. Embryol. Exp. Morphol.* **63**, 75–84.
- Navarro, P., Chambers, I., Karwacki-Neisius, V., Chureau, C., Morey, C., Rougeulle, C. and Avner, P.** (2008). Molecular coupling of Xist regulation and pluripotency. *Science* **321**, 1693–1695.
- Nesterova, T. B., Barton, S. C., Surani, M. A. and Brockdorff, N.** (2001). Loss of Xist imprinting in diploid parthenogenetic preimplantation embryos. *Dev. Biol.* **235**, 343–350.
- Nesterova, T. B., Johnston, C. M., Appanah, R., Newall, A. E. T., Godwin, J., Alexiou, M. and Brockdorff, N.** (2003). Skewing X chromosome choice by modulating sense transcription across the Xist locus. *Genes Dev.* **17**, 2177–2190.
- Niwa, H., Yamamura, K.-i. and Miyazaki, J.-i.** (1991). Efficient selection for high-expression transfectants with a novel eukaryotic vector. *Gene* **108**, 193–199.
- Norris, D. P., Patel, D., Kay, G. F., Penny, G. D., Brockdorff, N., Sheardown, S. A. and Rastan, S.** (1994). Evidence that random and imprinted Xist expression is controlled by preemptive methylation. *Cell* **77**, 41–51.
- Ohhata, T., Hoki, Y., Sasaki, H. and Sado, T.** (2008). Crucial role of antisense transcription across the Xist promoter in Tsix-mediated Xist chromatin modification. *Development* **135**, 227–235.
- Okabe, M., Ikawa, M., Kominami, K., Nakanishi, T. and Nishimune, Y.** (1997). 'Green mice' as a source of ubiquitous green cells. *FEBS Lett.* **407**, 313–319.
- Okamoto, I., Tan, S. and Takagi, N.** (2000). X-chromosome inactivation in XX androgenetic mouse embryos surviving implantation. *Development* **127**, 4137–4145.
- Okamoto, I., Otte, A. P., Allis, C. D., Reinberg, D. and Heard, E.** (2004). Epigenetic dynamics of imprinted X inactivation during early mouse development. *Science* **303**, 644–649.
- Penny, G. D., Kay, G. F., Sheardown, S. A., Rastan, S. and Brockdorff, N.** (1996). Requirement for Xist in X chromosome inactivation. *Nature* **379**, 131–137.
- Sado, T. and Sakaguchi, T.** (2013). Species-specific differences in X chromosome inactivation in mammals. *Reproduction* **146**, R131–R139.
- Sado, T., Tada, T. and Takagi, N.** (1996). Mosaic methylation of Xist gene before chromosome inactivation in undifferentiated female mouse embryonic stem and embryonic germ cells. *Dev. Dyn.* **205**, 421–434.
- Sado, T., Wang, Z., Sasaki, H. and Li, E.** (2001). Regulation of imprinted X-chromosome inactivation in mice by Tsix. *Development* **128**, 1275–1286.
- Sado, T., Hoki, Y. and Sasaki, H.** (2005). Tsix silences Xist through modification of chromatin structure. *Dev. Cell* **9**, 159–165.
- Sado, T., Hoki, Y. and Sasaki, H.** (2006). Tsix defective in splicing is competent to establish Xist silencing. *Development* **133**, 4925–4931.
- Sakai, K. and Miyazaki, J.-i.** (1997). A transgenic mouse line that retains Cre recombinase activity in mature oocytes irrespective of the cre transgene transmission. *Biochem. Biophys. Res. Commun.* **237**, 318–324.
- Savarese, F., Flahndorfer, K., Jaenisch, R., Busslinger, M. and Wutz, A.** (2006). Hematopoietic precursor cells transiently reestablish permissiveness for X inactivation. *Mol. Cell. Biol.* **26**, 7167–7177.
- Sugimoto, M. and Abe, K.** (2007). X chromosome reactivation initiates in nascent primordial germ cells in mice. *PLoS Genet.* **3**, e116.
- Tada, T., Obata, Y., Tada, M., Goto, Y., Nakatsuji, N., Tan, S., Kono, T. and Takagi, N.** (2000). Imprint switching for non-random X-chromosome inactivation during mouse oocyte growth. *Development* **127**, 3101–3105.
- Takagi, N. and Abe, K.** (1990). Detrimental effects of two active X chromosomes on early mouse development. *Development* **109**, 189–201.
- Takagi, N. and Sasaki, M.** (1975). Preferential inactivation of the paternally derived X chromosome in the extraembryonic membranes of the mouse. *Nature* **256**, 640–642.
- Takagi, N., Sugawara, O. and Sasaki, M.** (1982). Regional and temporal changes in the pattern of X-chromosome replication during the early post-implantation development of the female mouse. *Chromosoma* **85**, 275–286.
- Tease, C. and Fisher, G.** (1991). Two new X-autosome Robertsonian translocations in the mouse: I. Meiotic chromosome segregation in male hemizygotes and female heterozygotes. *Genet. Res.* **58**, 115–121.
- Williams, L. H., Kalantry, S., Starmer, J. and Magnuson, T.** (2011). Transcription precedes loss of Xist coating and depletion of H3K27me3 during X-chromosome reprogramming in the mouse inner cell mass. *Development* **138**, 2049–2057.
- Yamaguchi, S., Kurimoto, K., Yabuta, Y., Sasaki, H., Nakatsuji, N., Saitou, M. and Tada, T.** (2009). Conditional knockdown of Nanog induces apoptotic cell death in mouse migrating primordial germ cells. *Development* **136**, 4011–4020.
- Yoshimizu, T., Sugiyama, N., De Felice, M., Yeom, Y. I., Ohbo, K., Masuko, K., Obinata, M., Abe, K., Scholer, H. R. and Matsui, Y.** (1999). Germ-line-specific expression of the Oct-4/green fluorescent protein (GFP) transgene in mice. *Dev. Growth Differ.* **41**, 675–684.

Supplementary Materials and Methods

Construction of the targeting vector

Construction of the targeting vector, pCAG-CΔM20, and the generation of mice carrying the *Xist*^{CAG2L} allele were carried out as follows: a 4.6 kb EcoRI-BamHI fragment present in exon1 of the *Xist* gene was cloned into pBluescriptII SK(-), in which SalI and XhoI sites had been destroyed by double digestion and subsequent ligation of the compatible ends. A 4.4-kb EcoRI genomic fragment containing the major transcription start site of *Xist* was subsequently inserted at the EcoRI site of this plasmid in an appropriate orientation to derive pΔXS-EB9.0. PCR was carried out on genomic DNA using Mlu-Sal-21F(+)³⁷ and AS1634F as primers, and a product of about 900 bp was digested with MluI and XhoI and used to replace the endogenous MluI-XhoI fragment present in pΔXS-EB9.0 to generate pΔM20. In parallel, pCAG-CY NotI (a gift from Hitoshi Niwa), which has a floxed pac-EGFP-pA cassette downstream of the CAG promoter, was digested with NotI to release a 4.0-kb fragment containing the CAG promoter and the floxed cassette. Following the addition of a SalI linker at both ends, this fragment was cloned at the SalI site in pΔM20 in an appropriate orientation to generate pCAG-CΔM20.

Preparation of MEFs

$X^{CAG2L}X^{Rb(X.9)}$ and $X^{CAG2L}X^{JF1}$ fetuses were obtained at E13.5 from $X^{CAG2L}X$ females crossed with either $X^{Rb(X.9)}Y$ or JF1 males. $X^{Rb(X.9)}X^{CAG}$ and $X^{JF1}X^{CAG}$ fetuses were obtained at E13.5 by crossing [$X^{CAG2L}Y$; *Pgk2-cre*] males with either $X^{Rb(X.9)}X^{Rb(X.9)}$ or JF1 females. Following a removal of the head and internal organs, the carcass of each fetus placed in a 100-mm dish was minced into vary small pieces through an 18G hypodermic needle attached to a 2.5-ml syringe in 500 ul of PBS and cultured in DMEM/10% FBS for several days and passaged for expansion.

Primer sequences

Mlu-Sal-21F(+)+37:	5'-GGC CGT GAC GCG TCG ACA TGT GCC GG TTC TTC CGT GGT-3'
AS1634F	5'-GCG TAA CTG GCT CGA GAA TA-3'
XistEx7F21	5'-GCC CAG GTC ACA TTA TGG TT-3'
XistEx7R20	5'-CTC CAA TTT CTG GGC TCA AG-3'
18SRNA1	5'-TCA AGA ACG AAG TCG GAG GTT-3'
18SRNA2	5'-GCA CAT CTA AGG GCA TCA CAG-3'
Bx-CAG1113F	5'-AAA CTA CAA CCC CCC CTA CAC CCC CCT CCC-3'
Bx-CAG1686R	5'-TTG TTT AGG AGT TGT AGG AAA AAG AAG AAG-3'
Bx-CAG1646R	5'-GTA TGA ATA TGG TTA GTA GAG GTT TTA GAG-3'
XistPr2	5'-AAA TAT TCC CCC AAA ACT CCT TAA ATA A-3'
XistPr3	5'-GTT AAT TAA TGT AGA AGA ATT TTT AGT GTT TA-3'
XistPr4	5'-GGT TTG TTT AAG TAG AAG ATA TAT TGA AAT-3'

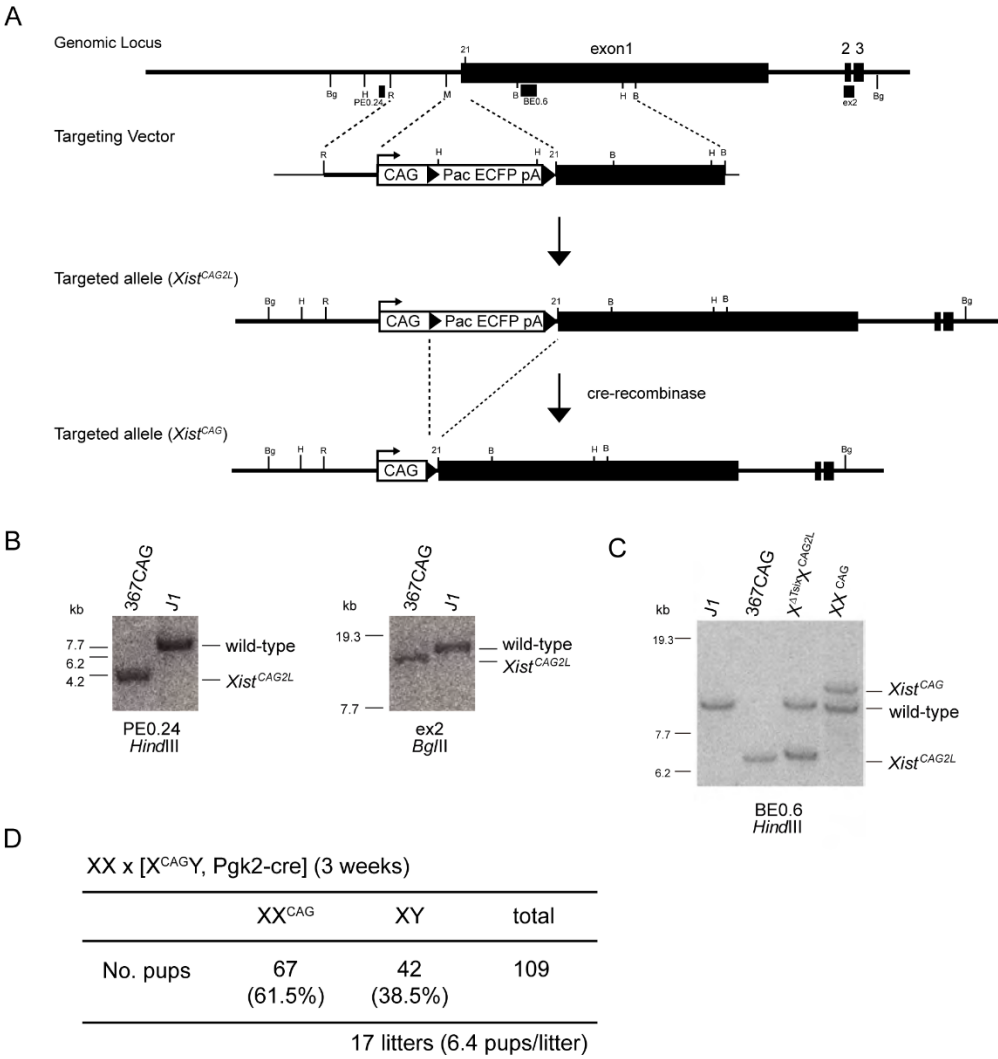


Fig. S1. Introduction of a constitutively active allele of *Xist* into the mouse

(A) the targeting scheme for generating the *Xist*^{CAG} allele. The endogenous *Xist* promoter was replaced with a CAG-Pac ECFP-pA cassette to produce the *Xist*^{CAG2L} allele, which would not produce *Xist* RNA. In the presence of cre recombinase, the *Xist*^{CAG2L} allele should be converted into the *Xist*^{CAG} allele, which in turn expresses *Xist* constitutively. The locations of the probes (PE0.24, BE0.6, and ex2) used for Southern blotting in B and C are indicated. H, *Hind*III; Bg, *Bgl*II; B, *Bam*HI; R, *Eco*RI; M, *Mlu*I. (B) Homologous recombination was confirmed by Southern blotting. 367CAG is the ES cell line harboring the correct targeting event. Genomic DNA digested with *Hind*III (left) and *Bgl*II (right) was probed with PE0.24 (Sado et al., 2006) and ex2 (a genomic fragment encoding *Xist* exon 2), respectively. (C) The presence of the respective allele was confirmed in mice. Genomic DNA digested with *Hind*III was probed with BE0.6 (Sado et al., 2005). (D) The number of pups recovered from a cross between wild-type females and X^{CAG2L}Y males carrying a P_{gk2}-cre transgene.

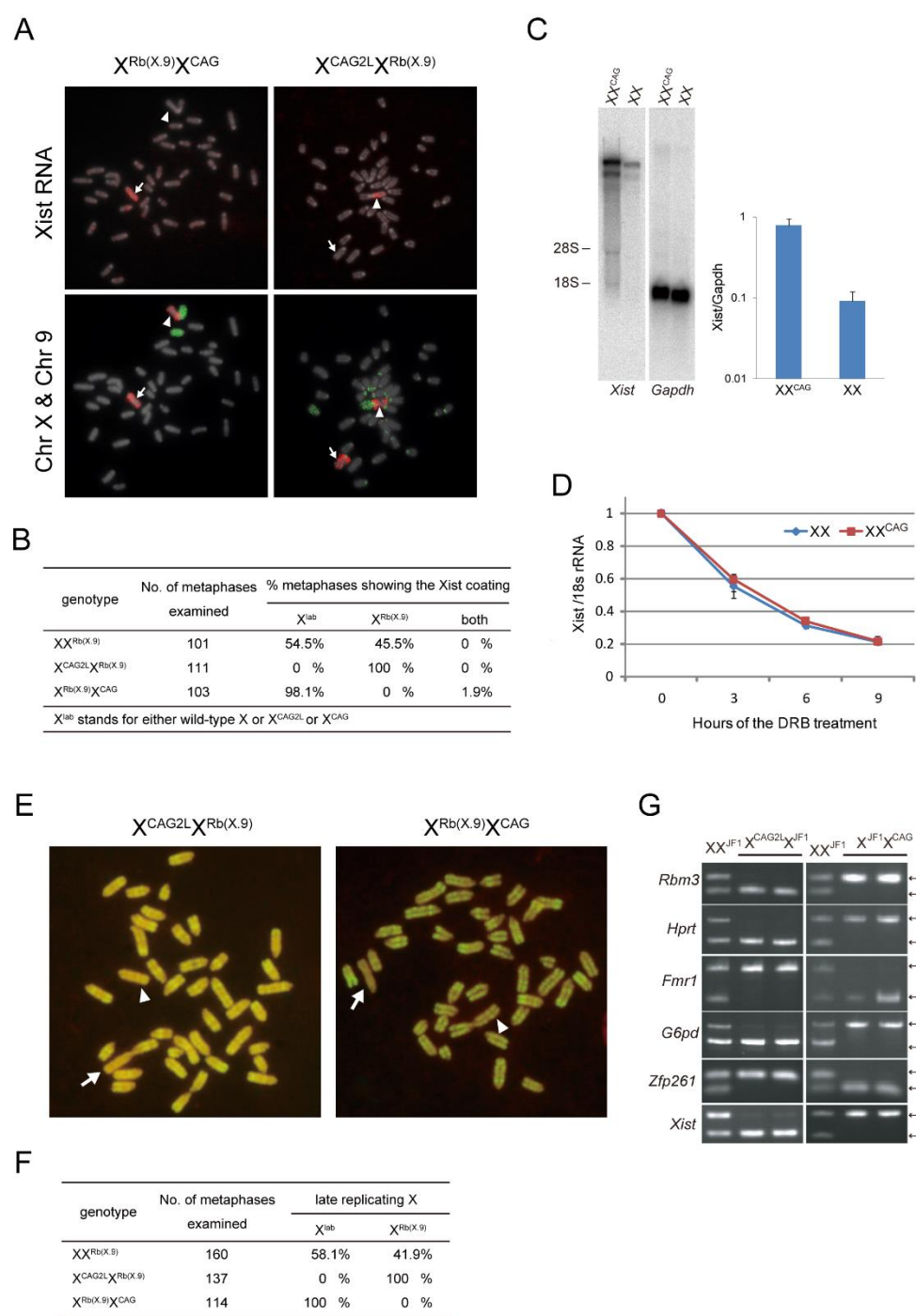


Fig. S2. The X chromosome carrying the *Xist*^{CAG} allele was preferentially inactivated in MEFs. (A) Representative images of RNA-FISH and subsequent chromosome painting in MEFs prepared from $X^{CAG2L}X^{Rb(X.9)}$ and $X^{Rb(X.9)}X^{CAG}$ fetuses. Upper panels show RNA-FISH detecting *Xist* RNA (red) accumulated on the X chromosome. DNA was counterstained with DAPI (blue). Lower panels show chromosome painting of the same metaphase spread examined by RNA-FISH in the upper

panels using probes specific for the X chromosome (red) and chromosome 9 (green). Arrows indicate morphologically normal wild-type or mutated X, whereas arrowheads indicate $X^{Rb(X.9)}$. **(B)** The prevalence of metaphases showing the *Xist* coating with either morphologically normal X (wild-type X, X^{CAG2L} , and X^{CAG}) or $X^{Rb(X.9)}$. The accumulation of *Xist* RNA was observed on either X chromosome in $XX^{Rb(X.9)}$ MEFs, reflecting random X-inactivation. In contrast, *Xist* RNA was found on $X^{Rb(X.9)}$ in $X^{CAG2L}X^{Rb(X.9)}$ MEFs, whereas it was essentially confined to the morphologically normal X^{CAG} in $X^{Rb(X.9)}X^{CAG}$ MEFs. A minor fraction in $X^{Rb(X.9)}X^{CAG}$ MEFs (1.9%) showed *Xist* coating on both X chromosomes. This may be due to the transmigration of overexpressed *Xist* RNA from the $Xist^{CAG}$ allele on X^{CAG} to the other X as previously reported by Jeon and Lee (Jeon and Lee, 2011). **(C)** The expression of *Xist* in XX and XX^{CAG} was examined by Northern blotting and quantitative RT-PCR. **(D)** The half-life assay of *Xist* RNA expressed from the $Xist^{CAG}$ allele. XX^{CAG} and XX MEFs were treated with DRB, an inhibitor of RNA polymerase II, and RNA was collected at different time points for qRT-PCR. The amount of *Xist* RNA present in MEFs prepared from XX and XX^{CAG} fetuses at each time point was measured relative to 18s ribosomal RNA by quantitative RT-PCR. **(E)** The replication patterns of chromosomes in $X^{CAG2L}X^{Rb(X.9)}$ and $X^{Rb(X.9)}X^{CAG}$ MEFs. $X^{Rb(X.9)}$ and X^{CAG} visualized as a pale chromosome in $X^{CAG2L}X^{Rb(X.9)}$ and $X^{Rb(X.9)}X^{CAG}$, respectively (arrows), were referred to as a typical inactive X chromosome. An active counterpart is indicated by arrowheads. 5-Bromo-2-deoxyuridine (BrdU) (100 μ g/ml) was incorporated into MEFs for 9 hours with Colcemid present at 100 ng/ml in the culture medium during the last hour. Chromosome spreads were stained with Acridine Orange. **(F)** Summary of the replication timing analysis in $XX^{Rb(X.9)}$, $X^{CAG2L}X^{Rb(X.9)}$, and $X^{Rb(X.9)}X^{CAG}$ MEFs, showing the prevalence of respective cells with either X^{Lab} referring to a morphologically normal X (wild-type X, X^{CAG2L} , and X^{CAG}) or $X^{Rb(X.9)}$, which replicated late in the S phase. **(G)** The allelic expression analysis of X-linked genes in MEFs derived from the F1 hybrid fetuses of JF and respective mutant mice. These MEFs allowed us to study the allelic expression of X-linked genes using restriction site polymorphisms between JF1 and laboratory strains. Six X-linked genes (*Rbm3*, *Hprt*, *Fmr1*, *G6pd*, *Zfp261*, and *Xist*) were analyzed by RT-PCR and the subsequent digestion of products with appropriate restriction enzymes. The origin of each fragment is shown on the right: X^{Lab} refers to either X^{CAG2L} , X^{CAG} , or wild-type X derived; X^{JF1} refers to the X derived from the JF1 strain.

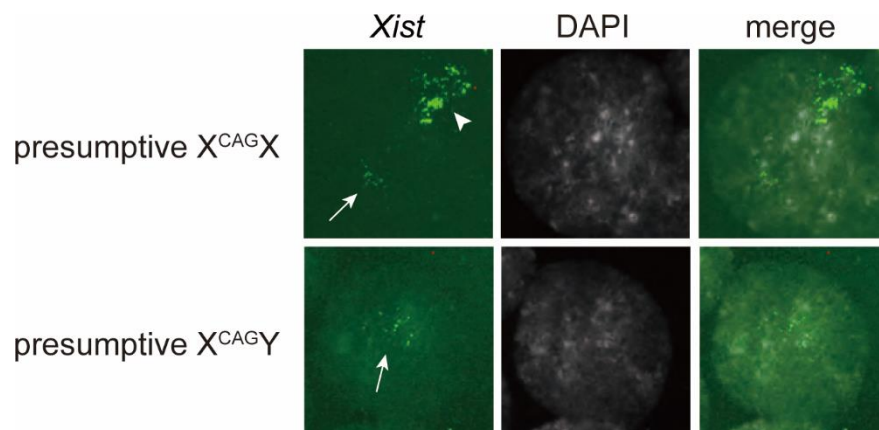


Fig. S3. RNA-FISH for *Xist* expression in 8-cell embryos recovered from a cross between XX^{CAG} females and wild-type males.

It is likely that the very faint scattered signals (arrows) represented very weak expression of from maternally inherited $Xist^{CAG}$. An arrowhead indicates a normal *Xist* cloud.

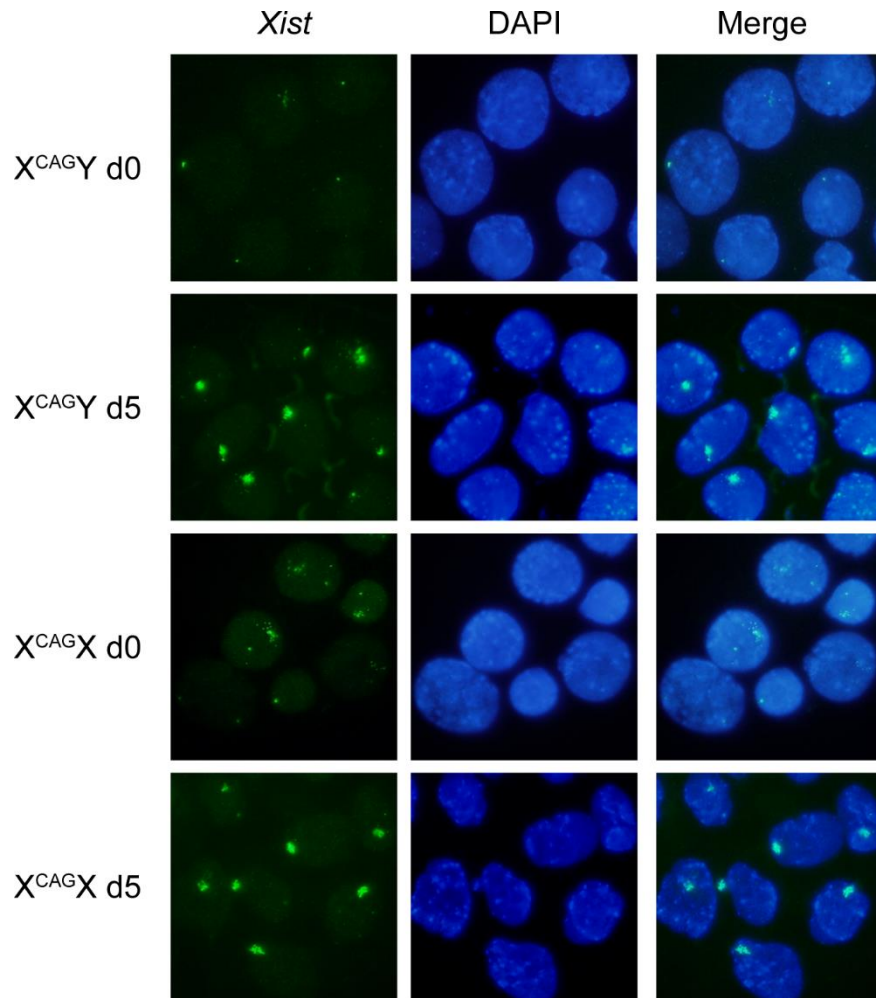


Fig. S4. RNA-FISH for Xist expression in X^{CAGY} and X^{CAGX} ES cells before (d0) and after (d5) differentiation.

The $Xist^{CAG}$ allele was upregulated in both male and female ES cells upon induction of differentiation. Undifferentiated ES cells were maintained in 2i medium, whereas differentiation was induced into Epiblast-like cells (EpiLCs) according to Hayashi et al (Hayashi et al., 2012).

- Hayashi, K., Ogushi, S., Kurimoto, K., Shimamoto, S., Ohta, H. and Saitou, M.** (2012). Offspring from oocytes derived from in vitro primordial germ cell-like cells in mice. *Science* **338**, 971-975.
- Jeon, Y. and Lee, J. T.** (2011). YY1 tethers Xist RNA to the inactive X nucleation center. *Cell* **146**, 119-133.
- Sado, T., Hoki, Y. and Sasaki, H.** (2005). Tsix silences Xist through modification of chromatin structure. *Developmental cell* **9**, 159-165.
- Sado, T., Hoki, Y. and Sasaki, H.** (2006). Tsix defective in splicing is competent to establish Xist silencing. *Development* **133**, 4925-4931.